6. R. J. Gryglewski, S. Chlopicki, J. Swies, P. Niezabitowski, *Ann. N. Y. Acad. Sci.* **748**, 194; discussion 206–7 (1995).
7. M. C. Kowala *et al.*, *Arterioscler. Thromb.* **13**, 435 (1993).
8. H. Sinzinger *et al.*, *Thromb. Haemostasis* **42**, 803 (1979).
9. J. N. Topper, J. Cai, D. Falb, M. A. Gimbrone Jr., *Proc. Natl. Acad. Sci. U.S.A.* **93**, 10417 (1996).
10. S. Moncada, R. Gryglewski, S. Bunting, J. R. Vane, *Nature* **263**, 663 (1976).
11. B. F. McAdam *et al.*, *Proc. Natl. Acad. Sci. U.S.A.* **96**, 272 (1999).
12. P. Akarasereenont, K. Techatraisak, A. Thaworn, S. Chotewuttakorn, *Inflamm. Res.* **49**, 460 (2000).
13. R. K. Tangirala, E. M. Rubin, W. Palinski, *J. Lipid Res.* **36**, 2320 (1995).
14. D. Pratico, R. K. Tangirala, D. J. Rader, J. Rokach, G. A. FitzGerald, *Nat. Med.* **4**, 1189 (1998).
15. Materials and methods are available as supporting material on *Science* Online.
16. K. M. Egan *et al.*, data not shown.
17. T. Munzel, I. B. Afanas'ev, A. L. Kleschyov, D. G. Harrison, *Arterioscler. Thromb. Vasc. Biol.* **22**, 1761 (2002).
18. H. A. Harris, J. A. Katzenellenbogen, B. S. Katzenellenbogen, *Endocrinology* **143**, 4172 (2002).
19. E. M. Malamas *et al.*, *J. Med. Chem.* **47**, 5021 (2004).
20. G. A. FitzGerald, *N. Engl. J. Med.* **351**, 17, 1709 (2004).
21. T. Murata *et al.*, *Nature* **388**, 678 (1997).
22. Q. Zhonghua *et al.*, *J. Clin. Invest.* **110**, 1, 61 (2002).
23. C. Y. Xiao *et al.*, *Circulation* **104**, 2210 (2001).
24. We thank H. Ischiropoulos and D. Fries (Children's Hospital of Philadelphia) for assistance. G.A.F. is on the Arcoxia Advisory Board for Merck and has consulted for or received grant support from Bayer, Boehringer Ingelhelim, CV Therapeutics, GlaxoSmithKline, Johnson and Johnson, Merck, Nicox, Novartis, Portola Pharmaceuticals, Pfizer, and Pharmacia/Searle in the past 5 years. This work was supported by grants from the NIH (HL70128 and HL62250).

Supporting Online Material
www.sciencemag.org/cgi/content/full/1103333/DC1
Materials and Methods
Fig. S1
Table S1

28 July 2004; accepted 3 November 2004
Published online 18 November 2004;
10.1126/science.1103333
Include this information when citing this paper.

Host-Parasite Coevolutionary Conflict Between *Arabidopsis* and Downy Mildew

Rebecca L. Allen,[1] Peter D. Bittner-Eddy,[1] Laura J. Grenville-Briggs,[1]* Julia C. Meitz,[1] Anne P. Rehmany,[1] Laura E. Rose,[2] Jim L. Beynon[1]†

Plants are constantly exposed to attack by an array of diverse pathogens but lack a somatically adaptive immune system. In spite of this, natural plant populations do not often suffer destructive disease epidemics. Elucidating how allelic diversity within plant genes that function to detect pathogens (resistance genes) counteracts changing structures of pathogen genes required for host invasion (pathogenicity effectors) is critical to our understanding of the dynamics of natural plant populations. The *RPP13* resistance gene is the most polymorphic gene analyzed to date in the model plant *Arabidopsis thaliana*. Here we report the cloning of the avirulence gene, *ATR13*, that triggers *RPP13*-mediated resistance, and we show that it too exhibits extreme levels of amino acid polymorphism. Evidence of diversifying selection visible in both components suggests that the host and pathogen may be locked in a coevolutionary conflict at these loci, where attempts to evade host resistance by the pathogen are matched by the development of new detection capabilities by the host.

Disease resistance in plants is a complex process that provides many potential barriers to pathogen invasion. Among the plant's defense arsenal are the disease resistance (*R*) genes, whose products trigger defense responses, such as localized host cell death, when challenged with pathogen isolates carrying matching avirulence genes (*1*). The largest class of *R* genes encodes proteins containing intra- or extracellular leucine-rich repeat (LRR) domains. LRR domains have been implicated in protein:protein interactions (*2*). However, direct interaction between an avirulence protein and its cognate R protein has been demonstrated in only a few host/pathogen systems (*3*, *4*).

Avirulence genes have been cloned from the fungal plant pathogens *Cladosporium fulvum* (*5*–*7*), *Magnaporthe grisea* (*8*), and *Melampsora lini* (*9*), but apart from the chitin-binding capacity of the Avr4 protein from *C. fulvum* (*10*), their roles in pathogenicity are unknown. We have recently shown the *RPP13* (*Recognition of Peronospora parasitica 13*) resistance gene from *Arabidopsis thaliana* to be the most polymorphic gene so far analyzed in this species (*11*). *RPP13* encodes a CC:NB:LRR (coiled coil: nucleotide binding site:leucine rich repeat) protein, predicted to be cytoplasmically located, and the extreme variability of the protein was shown to reside within the LRR domain (*11*, *12*). This is consistent with the LRR domain experiencing diversifying selection. One selective agent could be a pathogen species exhibiting comparable levels of polymorphism in the avirulence protein detected via RPP13. From the plant's perspective, there are two basic outcomes of a coevolutionary conflict: either a selective sweep in which a single allele of a resistance gene reaches high frequency in the plant population or balancing selection, in which a diverse cohort of resistance gene alleles is stably maintained (*13*). The large number (19 among 24 *Arabidopsis* accessions) of diverse alleles present at the *RPP13* locus implies that it is subject to balancing selection (*11*). Haldane's theory (*14*) suggests that coevolution of host and pathogen could lead to the maintenance of variation in both organisms. The interaction between *Arabidopsis* and the biotrophic oomycete *Hyaloperonospora parasitica* (formally *Peronospora parasitica*) is an excellent system in which to study such coevolution because both organisms coexist in extensive naturally occurring populations (*15*). Therefore, concomitant with extreme *RPP13* gene diversity, we hypothesize that balancing selection on the pathogen gene products recognized by these *R* genes [*ATR13* (*Arabidopsis thaliana recognised 13*)] would also result in the maintenance of a highly polymorphic population of *ATR13* alleles. Here we report the cloning of *ATR13* and show that it is indeed under intense diversifying selection consistent with host/parasite conflict occurring between these two species. Both *ATR13* and *RPP13* are subject to balancing selection.

We previously isolated a range of *H. parasitica* genes [*Ppat* (*Peronospora parasitica in Arabidopsis thaliana*)] that were up-regulated on infection of *Arabidopsis* (*16*). Mapping of the *Ppat* sequences among 206 F_2 progeny of a cross between *H. parasitica* isolates Maks9 (predicted to contain *ATR13*) and Emoy2 (predicted to contain *atr13*) revealed cosegregation of a single-copy gene, *Ppat17*, and *ATR13* (*17*). Therefore, *Ppat17* was an *ATR13* candidate.

Because no mechanism of genetic transformation has been established for *H. parasitica*, we developed a functional assay for *ATR13* recognition based on a biolistic ap-

[1]Warwick, HRI University of Warwick, Wellesbourne, Warwick, CV35 9EF, UK. [2]Department of Evolutionary Biology, University of Munich, Großhadernerstrasse 2, 82152 Planegg-Martinsried, Germany.

*Present address: College of Life Sciences and Medicine, University of Aberdeen, IMS, Foresterhill, Aberdeen, AB25 2ZD, UK.
†To whom correspondence should be addressed. E-mail: jim.beynon@warwick.ac.uk

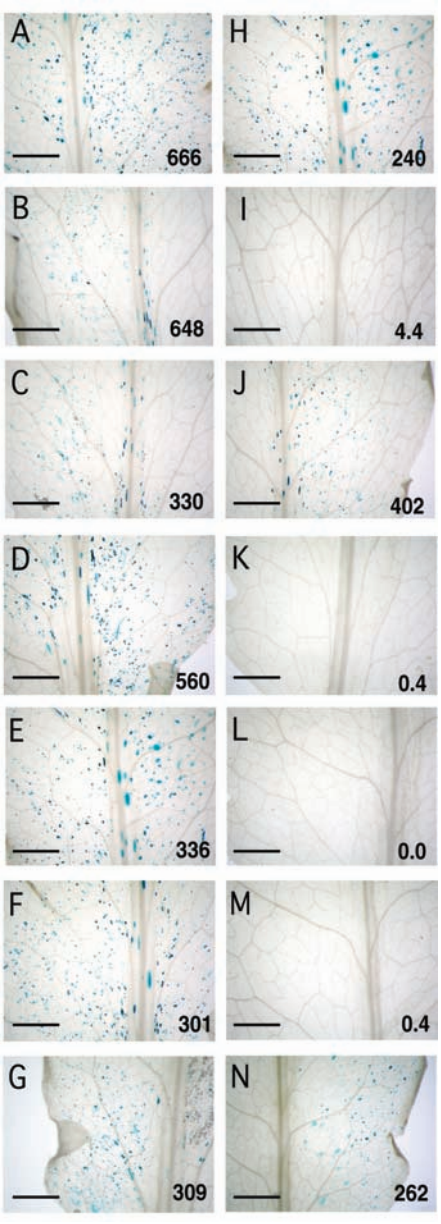

Fig. 1. Biolistic analysis of ATR13 alleles. (**A** to **G**) 8-week-old Col-5 leaves; (**H** to **N**) 8-week-old Col-5::*RPP13-Nd* leaves. (A) and (H) were bombarded with the control plasmid, pK2GW7, and the 35*S*::GUS plasmid; (B) and (I) were bombarded with the ATR13-Maks9 plasmid (without signal peptide) and the 35*S*::GUS plasmid; (C) and (J) were bombarded with the ATR13-Emoy2 plasmid (without signal peptide) and the 35*S*::GUS plasmid; (D) and (K) were bombarded with the ATR13-Aswa1 plasmid (with signal peptide) and the 35*S*::GUS plasmid; (E) and (L) were bombarded with the ATR13-Emco5 plasmid (with signal peptide) and the 35*S*::GUS plasmid; (F) and (M) were bombarded with the ATR13-Goco1 plasmid (with signal peptide) and the 35*S*::GUS plasmid; and (G) and (N) were bombarded with the ATR13-Hind4 plasmid (with signal peptide) and the 35*S*::GUS plasmid. Leaves were stained for β-glucuronidase activity and cleared with methanol. Numbers represent average numbers of blue-stained cells over five replicates. Scale bars, 2.5 mm.

proach. Three models could be proposed for the role of *ATR13* in the elicitation of plant cell death: (i) the presence of the ATR13 protein alone is sufficient; (ii) ATR13 acts in concert with monomorphic *H. parasitica* proteins; or (iii) ATR13 is an enzyme that produces a pathogen product, which triggers the hypersensitive reaction as in the case of *avrD* (*18*). Bombardment of *Arabidopsis* leaves with a plasmid carrying the bacterial *uidA* gene (*GUS*) fused to the 35*S* promoter results in blue-stained cells, in the presence of the substrate X-Gluc. (*17*). If model (i) is correct, then co-bombardment of *Arabidopsis* leaves expressing *RPP13* with the 35S::*GUS* plasmid and another carrying a 35*S*::*ATR13* fusion would result in cell death and consequently no *GUS* expression. Hence, we fused *Ppat17* to the 35*S* promoter and co-bombarded *Arabidopsis* accession Columbia, which contains an allele of *RPP13* that does not recognize Maks9 or Emoy2, and a Columbia transgenic line (Col5::*RPP13-Nd*) carrying the *RPP13* allele from the Niederzenz accession, which enables isolate-specific recognition of Maks9 but not Emoy2 (*12*, *19*). In an experiment using 35*S*::*GUS* and a control plasmid, large numbers of blue-stained cells were seen in both types of plant material (Fig. 1, A and H). However, when 35*S*::*GUS* and 35*S*::*Ppat17-Maks9* were co-bombarded, results similar to those with the control (648 blue-stained cells) were seen in Columbia, but this number was significantly reduced (4.4 blue-stained cells) in our Col5::*RPP13-Nd* line (Fig. 1, B and I). As a further test, we repeated the experiment using the Emoy2 allele of *Ppat17*, which would not be predicted to elicit a response from *RPP13-Nd*. In this experiment, the number of blue-stained cells was similar to the control in both plant lines (Fig. 1, C and J). We conclude that *Ppat17* is *ATR13*, and the protein it encodes is sufficient to trigger *RPP13*-dependent resistance.

To confirm the function of *ATR13* in vivo, we carried out in planta expression assays. We fused the *ATR13* Maks9 and Emoy2 alleles to a glucocorticoid-inducible plant promoter and generated transgenic Columbia plants and HRI3879, a selected recombinant inbred line containing *RPP13-Nd*, plants (*17*). In the presence of *RPP13-Nd*, the *ATR13-Maks9* gene caused wilting within 6 hours of dexamethasone application and death of the whole plant within 24 hours (Fig. 2, A and B). Induction of the Maks9 allele caused no phenotypic change in Columbia (Fig. 2, C and D). To confirm that ATR13-Maks9 protein was produced in these plants, they were crossed to Col5::*RPP13-Nd* and, as expected, all F_1 progeny tested died on induction of *ATR13-Maks9* (*20*). Induction of the Emoy2 *ATR13* allele in the presence or absence of *RPP13-Nd* resulted in no change in plant phenotype (*20*). These data imply that *RPP13* is expressed in a wide range of above-ground plant cell types and confirm the allele-specific nature of the interaction between *RPP13* and *ATR13-Maks9*.

ATR13-Maks9 encodes a 187–amino acid protein that shows no significant homology (BLASTP) (*21*) to other proteins but appears to have clear domain structures. ATR13-Maks9 has a heptad leucine/isoleucine repeat motif and, although reminiscent of coiled-coil domains that are involved in protein-protein interactions, this ATR13 domain is not predicted to lie within an α-

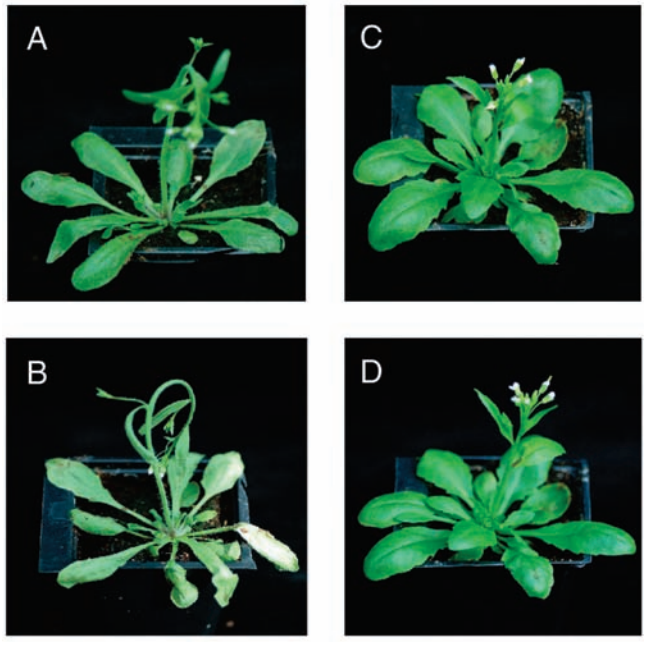

Fig. 2. Induced expression of *ATR13-Maks9* triggers a total cell death phenotype specific to *Arabidopsis* plants containing *RPP13-Nd*. *Arabidopsis* plant lines were transformed with *ATR13-Maks9* (minus signal peptide sequence) under the control of a dexamethasone-inducible promoter (*17*). Pictures were taken 6 hours (**A** and **C**) and 24 hours (**B** and **D**) after dexamethasone application. Representative T_3 homozygous transgenic HRI3879 plants (*RPP13-Nd*) (A) and (B) and Columbia (*RPP13-Col*) plants (C) and (D) are shown. Note the drooping inflorescence (A) and desiccated nature of the leaves in the transgenic HRI3879 plant (B). We observed similar responses when plants were transformed with full-length *ATR13-Maks9*.

helical structure (Fig. 3). An imperfect direct repeat of 4 × 11 amino acids lies between residues 93 and 136 and is followed by a C-terminal region within which no specific structures can be identified (Fig. 3). The program SignalP (*22*) reveals a high (P = 0.98) likelihood of a signal peptide being encoded at the N terminus with cleavage after the 19th amino acid (Fig. 3). This suggests that ATR13-Maks9 is secreted from *H. parasitica* during its growth in planta, which is consistent with it being exposed to and entering the plant cell where it could interact with RPP13-Nd.

The presence of an ATR13 signal peptide made no difference to the results obtained in the biolistic and in planta assays, and could be explained as a consequence of high levels of gene expression resulting in aberrant processing of ATR13 by the host's signal peptide recognition complex (*20*). Successful recognition of ATR13-Maks9 expressed without a signal peptide is consistent with its recognition by the intracellularly located RPP13-Nd, implying that ATR13-Maks9 is imported into the plant cell by an unidentified mechanism. Bacterial plant pathogens such as *Pseudomonas syringae* use the highly conserved type III secretion apparatus to transport their effector proteins across the plant plasma membrane (*23*), but an equivalent system has yet to be described in fungal or oomycete pathogens. The *AvrL567* gene family from *M. lini* encodes small potentially secreted proteins that have been shown to specifically trigger *R* gene–dependent cell death in flax lines carrying the cytoplasmically located L5, L6, and L7 resistance proteins (*9*). Both *H. parasitica* and *M. lini* possess specialized feeding structures called haustoria that form an intimate association with the plant plasma membrane (*24*), and potentially these are the sites at which these pathogens traffic their pathogenicity effectors.

RPP13-Nd initiates resistance reactions to the Aswa1, Emco5, and Goco1 isolates of *H. parasitica* in addition to Maks9, but not to Hind4 or Emoy2. To determine whether *ATR13* is central to this resistance, we cloned *ATR13* alleles from these additional isolates and tested their function using the biolistic assay. *ATR13-Aswa1*, *ATR13-Emco5*, and *ATR13-Goco1* all elicited an *RPP13-Nd*–dependent cell death response equivalent to that seen with *ATR13-Maks9* but *ATR13-Hind4* did not (Fig. 1, D to G and K to N). DNA sequence analysis revealed that all isolates carried a different *ATR13* allele than Maks9, but that of Emco5 and Goco1 were identical to each other (*25*). However, the overall structure of the predicted ATR13 proteins was retained (Fig. 3). Several amino acids varied within the heptad repeat region, but the heptad motif itself was conserved, suggesting a possible functional significance.

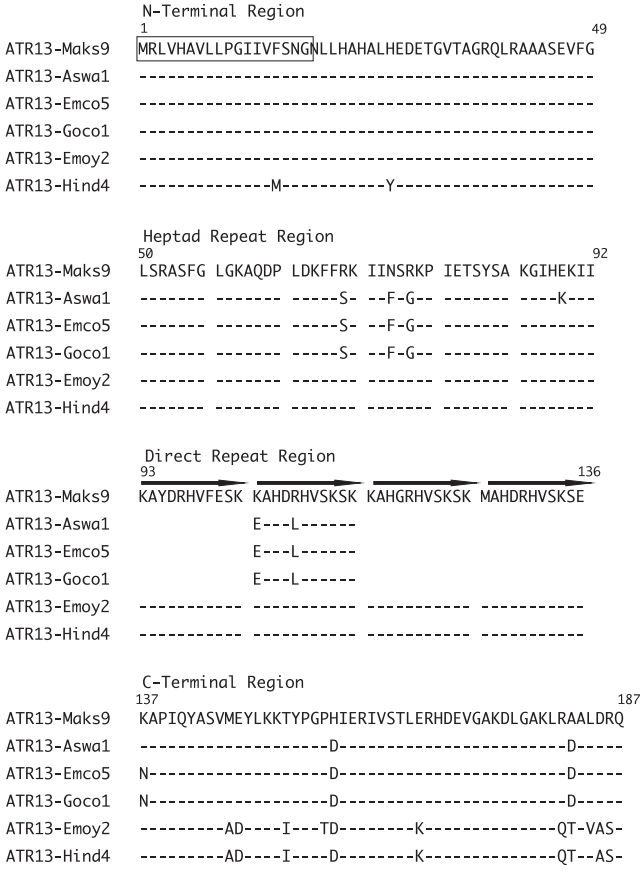

Fig. 3. Alignment of predicted proteins encoded by ATR13 alleles generated with Vector NTI. Dashes indicate amino acids identical to ATR13-Maks9. Amino acid residues differing from ATR13-Maks9 are shown. In the N-terminal region, the predicted signal peptide is boxed. In the direct repeat region, the repeats are shown by arrows. ATR13 from isolates Maks9, Aswa1, Emco5, and Goco1 triggers an *RPP13-Nd*–dependent resistance response, but ATR13 from isolates Emoy2 and Hind4 does not.

Surprisingly, ATR13 encoded by the alleles from Aswa1, Emco5, and Goco1 contained only one 11–amino acid repeat unit, indicating that repeats 1, 3, and 4 are dispensable for an *RPP13-Nd*–mediated resistance response. The *AvrBs3* avirulence gene family from *Xanthomonas campestris* pv. *vesicatoria* encodes proteins with a variable number of a 34–amino acid repeat motif, which was shown to determine specificity in its interaction with different plant *R* genes (*26*). In contrast, a repeated domain within ATR13 is not required for recognition by *RPP13-Nd*. However, we cannot preclude the possibility that the repeats have a role in determining recognition specificity via other *R* genes.

The Maks9 and Emoy2 alleles have identical DNA sequences throughout the N-terminal, heptad repeat, and direct repeat regions and only a single nucleotide polymorphism in 218 bases 5′ to translation initiation (*25*). This stretch of shared sequence identity between these two alleles over the first three-quarters of the protein, followed by a region of dissimilarity, uncovers two biologically relevant features. First, it reveals that the C-terminal portion of these two proteins is the region causing differential recognition by the *RPP13-Nd* allele. Second, it suggests that recombination has played a role in the evolutionary history of the *ATR13* gene. The inference of recombination is supported by permutation analysis, which detected a significantly long stretch of sequence identity between these two alleles (P = 0.008) (*27*).

RPP13 has evolved under intense diversifying selection (*11*) and as such offers a stark contrast to the related *Arabidopsis RPM1* gene where, presumably, invariant *Pseudomonas* effector proteins AvrRPM1 and AvrB do not appear to have driven the evolution of alternative *RPM1* alleles (*28*, *29*). If the evolution of *RPP13* were driven by its interaction with *H. parasitica*, then one would expect to see a similar evolutionary pattern in the matching avirulence gene. Among the five *ATR13* alleles, there are 26 nonsynonymous, two synonymous, and two indel polymorphisms. Based on a total of 351.5 nonsynonymous and 113.5 synonymous sites at *ATR13* (*30*), this represents a significant excess of nonsynonymous polymorphism relative to the neutral expectation (X^2 = 4.48, P = 0.034) and indicates selective maintenance of amino acid polymorphism at this locus. Amino acid polymorphism at ATR13 is not limited to differences between alleles that are recognized by RPP13-Nd and those that are not. Only eight amino acid differences are fixed between the two phenotypically distinct classes of alleles. There are nine amino acid and two indel polymorphisms among the three alleles recognized by RPP13-Nd, and four amino acid differences between the two alleles not recognized by RPP13-Nd. This is reminiscent of

the situation in *M. lini*, where two paralogs of the *AvrL567* gene, exhibiting significant amino acid variation, show differential recognition and response by the *L5*, *L6*, and *L7* flax resistance genes (*9*). However, *ATR13* alleles, showing not only extensive amino acid variation but also deletions of repeated domains, were equally effective in triggering resistance via *RPP13-Nd*. The high level of amino acid variation among alleles that are recognized by RPP13-Nd may indicate that these variants are selectively favored in *H. parasitica* parasitizing host populations not expressing *RPP13-Nd*. To confirm that not all *H. parasitica* genes are undergoing an equivalent extreme rate of change, we sequenced *Ppat5* from the same *H. parasitica* isolates. *Ppat5* encodes a dnaK-type molecular chaperone (*16*) and hence is likely to be under different selective pressures as compared to *ATR13*. DNA sequence analysis of *Ppat5* revealed only nine segregating polymorphisms across the 1983–base pair ORF and, in contrast to ATR13, only one of these is a nonsynonymous polymorphism (*25*).

Our study reveals the *RPP13/ATR13* plant/pathogen interaction to be an excellent model for studying the coevolution of resistance and avirulence genes within host and pathogen populations. The high levels of amino acid polymorphism relative to silent polymorphism in both plant and pathogen genes is consistent with a history of balancing selection operating at both loci. Within RPP13, it is the LRR domain that shows diversifying selection, whereas the rest of the gene shows selection for conservation of protein sequence (*11*, *12*). This study shows that the C-terminal domain of ATR13 plays a role in determining the specificity of interaction with RPP13, suggesting a direct interaction with the LRR domain. However, our initial yeast two-hybrid studies have not revealed a direct interaction between RPP13 and ATR13 (*31*). It is possible that different alleles of RPP13 recognize other pathogen proteins, and variation at this locus could be influenced by additional pathogen interactions, not necessarily limited to *H. parasitica*. Additionally, ATR13 may be detected by more than one host resistance gene, leading to increased selection for diversity in this protein. ATR13 must have a role in enabling *H. parasitica* to grow as an obligate biotrophic pathogen on *Arabidopsis*, and the elucidation of the roles of the observed motifs in planta will add substantially to our understanding of the mechanisms of biotrophic pathogenicity as well as those of host defense.

References and Notes

1. J. L. Dangl, J. D. Jones, *Nature* **411**, 826 (2001).
2. D. A. Jones, J. D. Jones, *Adv. Bot. Res.* **24**, 90 (1997).
3. Y. Jia, S. A. McAdams, G. T. Bryan, H. P. Hershey, B. Valent, *EMBO J.* **19**, 4004 (2000).
4. L. Deslandes *et al.*, *Proc. Natl. Acad. Sci. U.S.A.* **100**, 8024 (2003).
5. M. H. Joosten, T. J. Cozijnsen, P. J. De Wit, *Nature* **367**, 384 (1994).
6. J. A. van Kan, G. F. van den Ackerveken, P. J. de Wit, *Mol. Plant Microbe Interact.* **4**, 52 (1991).
7. R. Luderer, F. L. Takken, P. J. de Wit, M. H. Joosten, *Mol. Microbiol.* **45**, 875 (2002).
8. M. J. Orbach, L. Farrall, J. A. Sweigard, F. G. Chumley, B. Valent, *Plant Cell* **12**, 2019 (2000).
9. P. N. Dodds, G. J. Lawrence, A.-M. Catanzariti, M. A. Ayliffe, J. G. Ellis, *Plant Cell* **16**, 755 (2004).
10. N. Westerink, R. Roth, H. A. Van den Burg, P. J. De Wit, M. H. Joosten, *Mol. Plant Microbe Interact.* **15**, 1219 (2002).
11. L. E. Rose *et al.*, *Genetics* **166**, 1517 (2004).
12. P. D. Bittner-Eddy, I. R. Crute, E. B. Holub, J. L. Beynon, *Plant J.* **21**, 177 (2000).
13. R. M. May, R. M. Anderson, in *Coevolution*, D. J. Futuyma, M. Slatkin, Eds. (Sinauer, Sunderland, MA, 1983), pp. 189–206.
14. J. B. S. Haldane, *Ricerca Sci.* **19** (suppl. 1), 68 (1949).
15. E. B. Holub, J. L. Beynon, I. R. Crute, *Mol. Plant Microbe Interact.* **7**, 223 (1994).
16. P. D. Bittner-Eddy, R. L. Allen, A. P. Rehmany, P. Birch, J. L. Beynon, *Mol. Plant Pathol.* **4**, 501 (2003).
17. Materials and methods are available as supporting material on *Science* Online.
18. N. T. Keen *et al.*, *Mol. Plant Microbe Interact.* **3**, 112 (1990).
19. Fusions of *Ppat17* were made with and without the predicted signal peptide sequence and were tested in the biolistic and in planta assays. Similar results were obtained with both forms of the gene.
20. R. L. Allen *et al.*, data not shown.
21. S. F. Altschul *et al.*, *Nucleic Acids Res.* **25**, 3389 (1997).
22. J. D. H. Bendtsen, Nielsen, G. von Heijne, S. Brunak, *J. Mol. Biol.* **340**, 783 (2004).
23. Q. Jin, R. Thilmony, J. Zwiesler-Vollick, S. Y. He, *Microbes Infect.* **5**, 301 (2003).
24. M. Hahn, K. Mendgen, *Curr. Opin. Plant Biol.* **4**, 322 (2001).
25. See supplementary figures on *Science* Online.
26. G. Van den Ackerveken, E. Marois, U. Bonas, *Cell* **87**, 1307 (1996).
27. GENECONV: A computer package for the statistical detection of gene conversion, S. A. Sawyer (1999). Distributed by the author, Department of Mathematics, Washington University, St. Louis, MO, and available at www.math.wustl.edu/~sawyer. The Geneconv method was used to determine whether some regions of a pair of sequences had more consecutive identical polymorphic sites than would be expected by chance. This test assumes that mutations are neutral and independently distributed and that there has been no history of recombination between sequences. Permutation of the sequences was used to assign *P* values to the observed shared fragments and to evaluate their statistical significance.
28. M. R. Grant *et al.*, *Science* **269**, 843 (1995).
29. E. A. Stahl, G. Dwyer, R. Mauricio, M. Kreitman, J. Bergelson, *Nature* **400**, 667 (1999).
30. J. Rozas, J. C. Sánchez-DelBarrio, X. Messeguer, R. Rozas, *Bioinformatics* **19**, 2496 (2003).
31. R. L. Allen, S. Hall, J. L. Beynon, unpublished results.

32. We thank H. Kaminaka and J. Dangl for allowing us to use pBDex; S. Bright, V. Buchanan-Wollaston, S. Hall, and B. Thomas for critical review of the manuscript; and E. Holub for provision of pathogen isolates. Supported by the Biotechnology and Biological Sciences Research Council and the Department of Environment, Food and Rural Affairs (under license PHL275/4864).

Supporting Online Material

www.sciencemag.org/cgi/content/full/306/5703/1957/DC1
Materials and Methods
Figs. S1 and S2
References

13 August 2004; accepted 22 October 2004
10.1126/science.1104022

Leading-Edge Vortex Lifts Swifts

J. J. Videler,[1,2]* E. J. Stamhuis,[1] G. D. E. Povel[2]

The current understanding of how birds fly must be revised, because birds use their hand-wings in an unconventional way to generate lift and drag. Physical models of a common swift wing in gliding posture with a 60° sweep of the sharp hand-wing leading edge were tested in a water tunnel. Interactions with the flow were measured quantitatively with digital particle image velocimetry at Reynolds numbers realistic for the gliding flight of a swift between 3750 and 37,500. The results show that gliding swifts can generate stable leading-edge vortices at small (5° to 10°) angles of attack. We suggest that the flow around the arm-wings of most birds can remain conventionally attached, whereas the swept-back hand-wings generate lift with leading-edge vortices.

The discovery of leading-edge vortices (LEVs) on the wings of insects in flight greatly advanced the knowledge of their dominant lift-generating mechanisms (*1, 2, 3*). Sharp leading edges induce high lift production through flow separation with vortical flow attached to the upper surface of insect wings during flapping and gliding.

[1]Department of Marine Biology (Experimental Marine Zoology Group), Groningen University, Post Office Box 14, 9750 AA, Haren, Netherlands. [2]Evolutionary Mechanics, Institute of Biology, Leiden University, Post Office Box 9516, 2300 RA Leiden, Netherlands.

*To whom correspondence should be addressed. E-mail: j.j.videler@biol.rug.nl

Avian wings, unlike insect and aircraft wings, consist of two distinct parts: an arm-wing and a hand-wing. Cross sections through arm-wings show conventional aerodynamic profiles with a rounded leading edge. In contrast, the leading edge of hand-wings is sharp, because it is the edge of the narrow vane of the outermost primary feather. Birds often use the hand-wings in a swept-back position forming a V-shaped wing configuration. Here, we apply digital particle image velocimetry (DPIV) (*4*, *5*) using models of the wing of the common swift (*Apus apus*), tested in a water tunnel, to investigate the lift generated by swept-back hand-wings of gliding birds (Fig. 1).